VNIR image simulation based on low-level flight image data

Dongying Zhang (张冬英)[1,2*], Weining Yi (易维宁)[1], Jin Hong (洪 津)[1], Lili Du (杜丽丽)[1], Wei Fang (方 薇)[3], and Yanli Qiao (乔延利)[1]

[1]*Key Laboratory of Optical Calibration and Characterization, Chinese Academy of Sciences, Hefei 230031, China*

[2]*Information Department, Artillery Academy of PLA, Hefei 230031, China*

[3]*Institute of Intelligent Machines, Chinese Academy of Sciences, Hefei 230031, China*

[*]*E-mail: emilyzdy@aiofm.ac.cn*

Received July 16, 2009

A simulation method for visible and near infrared (VNIR) image is mentioned. The VNIR image obtained by low-level flight is adopted as data resource. After atmospheric correction, the ground reflectivity can be deducted. The simulation method consists of four steps: radiative transfer, spatial resolution, modulation transfer function, and noise simulation. The image of satellite-borne or high-level air-borne sensor could be generated by the simulation method from VNIR image. Experiment is carried out to test the method using an airship as platform. The resulting simulated image is compared to the image with quickbird panchromatic band. The result shows that simulation images enables one to effectively reproduce the entire process of remote sensing of the Earth. The method can be used to simulate VNIR image at satellite level at the same area and the same wavelength.

OCIS codes: 010.0280, 100.2000, 280.4991.

doi: 10.3788/COL20100804.0345.

The simulation of remote sensing data has significant importance for the development, optimization, calibration, test, and application of optoelectronic instruments as well as the interpretation of their data products[1]. Simulated image can provide a practical alternative to field measurements, for which it is typically expensive, time consuming, and impractical to cover the full range of anticipated atmospheric and surface conditions[2]. And sometimes it is the only way for the adaptation and optimization of a sensor and its observation condition's algorithm. Thus, it becomes an accurate, robust, and efficient means for simulating the interactions among sun, earth, target, and sensor.

For a long time, the evaluation of electro-optical systems performance was usually conducted by mathematical models. In the models the targets and background were often set simply. The spectral reflectivities and emissivities of different materials were identified by category type and stored in database. Then the surface reflectance properties were assigned on a pixel-by-pixel basis[3]. Taking account with the demand of high precision data, these simple models appeared more and more insufficient for simulation. Recently, a new method which simulated satellite images derived from the low-level flight images was brought out.

The simulation process is as follows. Firstly the visible and near infrared (VNIR) images are taken by two charge-coupled device (CCD) cameras carried on a low-level airship. Secondly, the spectral ground reflectivity is retrieved by radiative transfer model or by empirical linear method. Finally, the atmospheric influence of the radiation, spatial resolution, modulation transfer function (MTF), and signal-to-noise ratio (SNR) of the sensor on high level are taken into account.

Figure 1 depicts the general data flow diagram of the simulation method. Images obtained at low-level airship consist of objects in bands from visible to near infrared (NIR). The aerosol optical depth (sometimes visibility) and reflectivity measured synchronously are used for atmospheric correction. Hence images at ground could be calculated. Each pixel of ground image represents a reflectance at a certain wavelength. Then satellite images could be generagted at different atmosphere models and different aerosol models through the following four steps: radiative transfer simulation, spatial resolution simulation, MTF simulation, and noise simulation.

The radiative transfer describes the influence of the Earth's atmosphere on the solar irradiance. According to radiative transfer equation, the radiance at a satellite sensor in bands from visible to NIR can be calculated by

$$L_{\mathrm{a}} = L_{\mathrm{p}} + \frac{\tau \cdot \rho \cdot E_{\mathrm{g}}}{\pi}, \tag{1}$$

where L_{a} is the apparent radiance at the sensor, L_{p} is the path radiance, ρ is the reflectance of object at ground level, E_{g} is the irradiance at ground level, and τ is the global gas transmittance. $L_{\mathrm{p}}, E_{\mathrm{g}}$, and τ could be

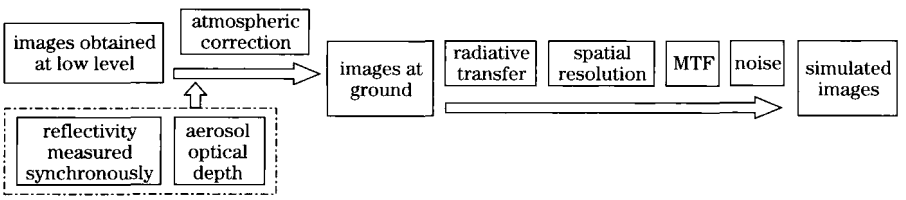

Fig. 1. Schematic diagram of data flow.

calculated by radiative transfer code for a given band, a set of input parameters describing the view and illumination opto-geometry, and atmosphere etc. In this method, a software model of moderate resolution transmission (MODTRAN)[4] is adopted here. It is the successor of the atmospheric Tadiative transfer model LOWTRAN 7 (Kneizys *et al.*, 1988) and is publicly available. It contains a large number of spectral databases of the extraterrestrial solar irradiance and the absorption of all relevant atmospheric gases with a high spectral resolution. Its maximum spectral resolution is 2 cm^{-1}. The incorporated DISORT algorithm[5] can be applied for accurate multiple scattering calculations, and the multilayer structure of the model enables realistic simulation of spectral radiances over the solar-reflective and thermal windows. The atmosphere is treated as a stack of up to 33 atmospheric layers, from 0 to 100 km altitude. Ten standard atmosphere models himself can be used, or the user can supply a customized atmospheric profile based on direct measurements or radiosonde profiles. Twelve aerosol models can also be used to simulate the effects of dust, clouds, or other particulates in the path. In this method, MODTRAN calculates the spectral transmittance, path radiance, and ground irradiance from ground to satelitte sensor by an input parameter which consists of atmosphere and aerosol type, visibility, surface and sensor altitude, view zenith angle, relative azimuth angle, and solar zenith angle.

Spatial resolution simulation converts the input image's ground sampling distance (GSD) to the desired sensor's GSD. GSD which refers to the size of an image pixel is a function of the instantaneous field of view (IFOV) and altitude of the sensor[6]. The aim of simulation is to generate a low-resolution GSD image from an original high-resolution GSD image by spatial degradation which utilizes resampling techniques to simulate spatially the desired image product. Resampling is performed from a block of $N \times N$ pixels in the original image to degrade a simple pixel in new image:

$$g(x,y) = \frac{1}{M} \sum_{i=1,j=1}^{N} f(x_i, y_i) H(x_i, y_i), \tag{2}$$

where $g(x,y)$ is the image after resampling, $f(x,y)$ is the image before resampling, $H(x,y)$ is a weighted function, M is the sum of weighted function.

The image quality of the optical instrument as well as the distance to the Earth and the viewing angle determine the effective ground resolution, usually expressed by MTF which describes the normalized response as a function of spatial frequency. For the image simulations, no spectral dependence of the MTF is assumed after applying the appropriate spatial resolution simulation.

For a linear restoration problem, the original image is degraded by a convolution operation with the point spread function of the degradation, thus the measured image is given by

$$g(x,y) = f(x,y) * h(x,y), \tag{3}$$

where $*$ is convolution product, $f(x,y)$ is the original image, $h(x,y)$ is the impulse response of the sensor, and $g(x,y)$ is the output image.

A classical way to deal with a convolution product is to apply a Fourier transform which leads to

$$G(\mu,\upsilon) = F(\mu,\upsilon) M(\mu,\upsilon), \tag{4}$$

where (μ,υ) is spatial frequency, $F(\mu,\upsilon)$ is the Fourier transform of the original image, $G(\mu,\upsilon)$ is the Fourier transform of the output image, $M(\mu,\upsilon)$ is the MTF. The blurred output image is obtained by Eq. (4).

The noise effects must be taken into account. The random noise consists of shot noise, thermal noise, read noise, quantization error, and relative calibration error[7,8]. Although some of the noise may be dependent on the signal (shot noise and calibration error), some are uncorrelated with the signal and could be added directly. Also, each noise is assumed to be independent of the others and uncorrelated with the spectral band. In this method, the noise is modeled as zero mean random processes. Thus noise is simulated by adding to each band of the radiance image with a matrix of random numbers which has a zero mean and a standard deviation that equals the desired sensor's SNR at each pixel.

As an example of using the proposed method, the simulation of the images was verified by a field experiment. Two imaging systems were loaded on an airship (Fig. 2) and flown at 500 m above sea level in the summer of 2007. One imaging system consisted of an optic lens, a liquid crystal tunable filter, and a CCD camera[9] whose wave band was from 420 to 720 nm with a step of 20 nm. The other imaging system consisted of an optic lens, a motor-driven filter wheel, and a CCD camera which carried 3 NIR and a pan-chromatic wave bands. Thus image cubes from visible to NIR were collected.

With the image cubes described above, data analysis and simulation were performed to evaluate the sensor performance of the satellite. Figure 3 shows simulation images and the pan-chromatic image of quickbird obtained at 2006. Firstly, the pan-chromatic image of data cube was selected to evaluate image at an altitude of 450 km with the following parameters: the atmosphere model is midLatitude summer, the aerosol model is rural, vis=23 km. Secondly, spatial degradation was matched to the 0.6-m GSD of the quickbird's pan-chromatic band. And the MTF of pan-chromatic band of quickbird was applied. Finally, a zero mean and 5% standard deviation random noise was added to the image. Thus the final image was generated. Table 1 shows the difference of digital numbers

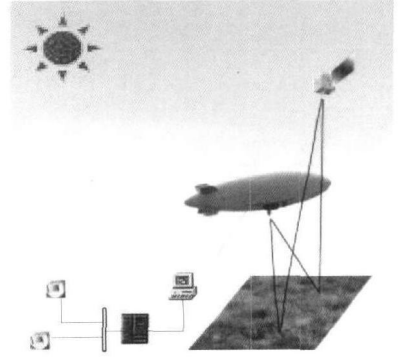

Fig. 2. Schematic of a field experiment.

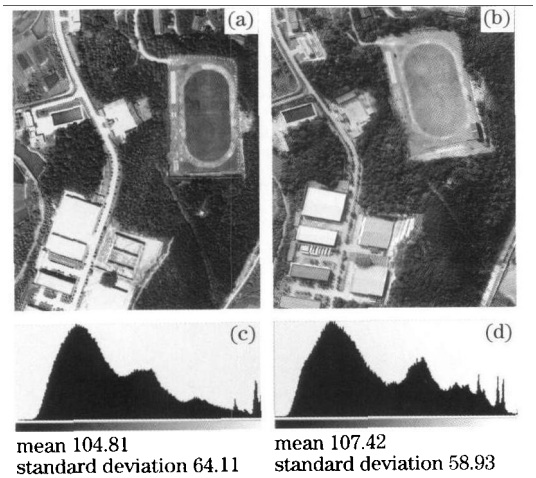

Fig. 3. Simulation results. (a) Quickbird image; (b) simulated image; (c) histogram of quickbird image; (d) histogram of simulated image.

Table 1. Difference of DNs between Simulated Image and Quickbird Image

DN	Quickbird	Simulated Image	Difference
Mean	104.81	107.42	2.61
Standard Deviation	64.11	58.93	5.18

between simulated image and the image of quickbird's pan-chromatic band.

From Table 1, we can see that the difference is small. The maximum similarity of two images is 83.3% according to template matching computation. The comparison result indicates that the method can be used to simulate VNIR image at satellite level at the same ground area and the same wavelength.

The main causes of errors are the atmosphere, the characteristic of satelitte sensor, and the data resource. It is better to define the atmosphere model and aerosol model by user's long-period observation of wind speed, humidity, press, and aerosol optic thickness than applying MODTRAN model. It will increase the precision of the simulation. The other way is to use the real sensor's characteristic such as GSD, spectral response function, MTF, and noise (model and SNR) in order to enhance the precision.

In conclusion, we propose a four-step simulation method for low-level flight VNIR image. With this method, satellite-borne or high-level air-borne image can be generated with the quality comparable to that of quickbird pan-chromatic image. This method can be used to simulate VNIR image at satellite level at the same area and the same wavelength.

This work was supported by the Directional Innovation Project of Chinese Academy of Sciences under Grant No. KGCX-SW-413.

References

1. A. Börner, L. Wiest, P. Keller, R. Reulke, R. Richter, M. Schaepman, and D. Schläpfer, ISPRS Journal of Photogrammetry and Remote Sensing **55,** 299 (2001).
2. S. Richtsmeier, R. Sundberg, A. Berk, S. Adler-Golden, and R. Haren, Proc. SPIE **5425,** 530 (2004).
3. R. Sundberg, A. Berk, S. Richtsmeier, S. Adler-Golden, and R. Haren, Proc. SPIE **5234,** 252 (2004).
4. A. Berk, G. P. Anderson, P. K. Acharya, J. H. Chetwynd, L. S. Bernstein, E. P. Shettle, M. W. Matthew, and S. M. Adler-Golden, "Modtran4 User's Manual" Air Force Research Laboratory Report (June 1999).
5. K. Stamnes, S.-C. Tsay, W. Wiscombe, and K. Jayaweera, Appl. Opt. **27,** 2502 (1988).
6. V. Zanoni, B. Davis, R. Ryan, G. Gasser, and S. Blonski, in *Proceedings of ISPRS Commission Mid-Term Symposium 2002* WGI/2 (2002).
7. X. Ding, Y. Li, Q. Yu, and W. Feng, Acta Opt. Sin. (in Chinese) **28,** 99 (2008).
8. J. Huang and M. Shen, Acta Opt. Sin. (in Chinese) **28,** 1686 (2008).
9. D. Zhang, J. Hong, W. Tang, W. Yang, J. Luo, Y. Qiao, and X. Zhang, Spectrosc. Spect. Anal. (in Chinese) **28,** 2455 (2008).